Volume crystallization and microwave dielectric properties of indialite/cordierite glass by TiO_2 addition

Hitoshi Ohsato[1,2*], Jobin Varghese[1,3*], Akinori Kan[4], Jeong Seog Kim[5], Isao Kagomiya[6], Hirotaka Ogawa[3], Mailadil Thomas. Sebastian[1], and Heli Jantunen[1]

[1]Microeoectronics Research Unit, Faculty of Information Technology and Electrical Engineering, University of Oulu, 90014 Oulu, Finland

[2]Department of Research, Nagoya Industrial Science Research Institute, Nagoya 464-0819, Japan

[3]Microsystems, LTCC and HTCC, Fraunhofer IKTS, Winterbergstraße 28, Dresden, 01277, Germany.

[4]Faculty of Science and Technology, Meijo University, Nagoya 468-8502, Japan

[5]Department of Material Science and Engineering, Hoseo University, Asan 336-795, Korea

[6]Department of Material Science and Engineering, Nagoya Institute of Technology, Nagoya 466-8555, Japan

ohsato.hitoshi@gmail.com

jobin.var@gmail.com

Abstract

Indialite/cordierite ($Mg_2Al_4Si_5O_{18}$) glass-ceramics with a low dielectric constant of 4.7 and a high *Qf* of > 200 × 10^3 GHz are predicted for use as micro/millimeter-wave materials in the fifth generation (5G) mobile communication systems. The glass-ceramics have a serious cracking problem caused by the anisotropic crystal growth during the surface crystallization. In this paper, the cracking was prevented by adding TiO_2 which acts as a seed. The glass-ceramics produced without cracking were composed of spherical crystals of approximately 10 μm diameter, formed by volume crystallization. Precipitated phases of the glass-ceramics crystallized at 1200 to 1350 °C/10 h and 20 h were indialite, cordierite, Al_2TiO_5 and rutile. The glass-ceramics crystallized for 10 h were analyzed by the Rietveld method. Indialite precipitated as an intermediate metastable compound at the lower temperature of 1200 °C and transformed to cordierite at the crystallization temperature. The reaction between cordierite and TiO_2 produced the new Al_2TiO_5 phase. The amounts of Al_2TiO_5 and rutile affected the microwave dielectric properties. In particular, the amount of rutile affected the *TCf*. In the cases of 10 wt. % added TiO_2, and the crystallized at 1250 °C for 10/20 h the *TCf* values were improved to -2/-8 ppm/°C.

Keywords: Volume crystallization; Indialite; Microwave dielectric properties; XRPD; Refinement; Glass ceramics

1. Introduction

Materials with a high-quality factor *Qf* and a low dielectric constant ε_r are a requirement in the fifth generation (5G) mobile communication systems for high-speed data transfer and low latency (time delay)[1-3]. The data transfer rate is proportional to the frequency as reported by IEEE, and so a high frequency such as the millimeter-wave frequency could be used for the 5G mobile communication system[4-5]. In general, at high frequencies dielectric losses are increased in conventional materials due to the increase in wave number. Hence high *Qf* values are also targeted for new materials[1]. On the other hand, when the wavelength is very small (of millimeter order) for the fabrication of the resonator, the low dielectric constant ε_r is mandatory for shortness of the wave-length λ_d in dielectrics according to the following equation[6-7]:

$$\lambda_d = \lambda_0 / \sqrt{\varepsilon_r}$$

Here, λ_0 is the wavelength in a vacuum.

In addition, the low dielectric constant also reduces the time delay T_{PD} according to the following equation[1,8]:

$$T_{PD} = \sqrt{\varepsilon_r}/c$$

Where c is the velocity of light.

Silicate family materials are possible candidates for these applications, having a low dielectric constant and high *Qf*[9]. For example, forsterite[10-16]($\varepsilon_r = 5.6$, $Qf = 270\times 10^3$

GHz), willemite[17-18] (ε_r = 6.5, Qf = 219× 10^3GHz) and diopside[19] (ε_r = 7.6, Qf = 121× 10^3GHz) [20]. The low dielectric constant is based on the covalency of SiO_4, which has 55% covalency and 45% ionisity[21]. However, their temperature coefficient of resonant frequency *TCf* is large and negative such as -65 ppm/°C of forsterite[11] or -61 ppm/°C of willemite[17]. Terada *et al.* focused on the *TCf* of cordierite with a near-zero value of -24 ppm/°C[22,23]. They improved the *Qf* value of cordierite using Ni doping, and found that cordierite transformed to indialite, a polymorph of cordierite[22]. Indialite, with the *P*6/*mcc* (No.192) space group, is a high-temperature form of cordierite with a *Cccm* (No. 66) space group based on order-disorder transition[24]. It is difficult to synthesise indialite by solid state reaction because of the transition temperature located near to the incongruent melting temperature of 1465 °C [25]. On the other hand, it is known that indialite is precipitated as an intermediate phase during crystallization from glass to cordierite[26]. Consequently, the authors performed the crystallization of cordierite glass for the formation of indialite. Crystallized glass pellets showed good microwave dielectric characteristics of ε_r = 4.7, and Qf > 200× 10^3GHz, and were fabricated from glass cast from melts at 1550 °C [27, 28].

On the crystallization, two major problems, such as deformation and cracking, were presented in a previous paper[28]. The deformation, as shown in Fig. 1(a)(i), may be due to

the formation of glass phases as shown in the previous paper [28], and the cracking as shown in Fig. 1(b)(i), is due to anisotropic crystal growths that are crystallized from different glass block surfaces, as shown in Fig. 2(a) [28]. This phenomenon is called "surface crystallization". These crystals, grown from different surfaces, meet at the end of the crystal growth, and cause cracks because of different thermal expansions, i.e. positive for *c*-axis of elongation and negative for *a*-axis[29]. So, the cracking could be the result of strain during cooling. In this work, the authors prevented these problems by the addition of TiO_2 as a dopant (nucleating agent), which also had the effect of adjusting the *TCf*. Moreover, the effects of the TiO_2 addition on microwave dielectrics were investigated together with the identification of the precipitated phases and the microwave dielectric properties.

2. Experimental Procedure

Mixed powders with cordierite composition $Mg_2Al_4Si_5O_{18}$ were prepared using high-purity raw materials: MgO, Al_2O_3, SiO_2, TiO_2 (> 99.9 wt. % purity) as described in Ohsato's previous published paper[27]. The mixed powders were melted at 1550 °C, clarified at 1600 °C/1 h, and cast in a graphite mold of ϕ 10 x 30 mm size. The glass rods were annealed to relieve the thermal stress in the glass at a temperature below the glass transition temperature (T_g) [30]. Glass pellets of ϕ 10 x 6 mm size were cut and crystallized

at 1200 - 1350 °C/10 and 20 h. The crystallized samples were polished to a thickness of up to half of the diameter, and analyzed using optical polarizing microscopy photos (ZEISS, Axioplan 2), scanning electron microscopy (SEM) images (FEI, Quanta 200 FEG), and X-ray powder diffraction (XRPD) patterns (Bruker, D8), The microwave dielectric properties ε_r and *TCf* were measured by the Hakki and Coleman method and *Qf* by the resonant cavity method.[31-32]. The crystalline secondary phase ratios of the precipitated phases were determined by the Rietveld method with Fullprof software[33] using XRPD data, which was taken by step scanning at 0.02° for 10 s/step using radiation generated by an X-ray tube of 40 KV 20 mA.

3. Results and Discussion

Table 1 shows the data relating to all samples with various percentages of TiO_2 (0, 10 and 20 wt.%) added to indialite/cordierite glass-ceramics crystallized at 1200 to 1350 °C/ 10 and 20 h, together with their associated microwave dielectric properties and reported materials with relative permittivity less than 5 and Qf < $20*10^3$ GHz [34-39]. The effects of the addition of TiO_2 are discussed in this paper. Figs. 1(a) and (b) show photographs of the crystallized pellets of indialite/cordierite glass-ceramics comparing **those without TiO_2 added and** those with 10/20 wt.% TiO_2. The images were obtained by optical stereo microscope and optical microscope, respectively.

These results helped to clarify the effects of TiO_2 addition. Although the pellets were deformed and cracked in the case of 0% TiO_2 addition as shown in Fig. 1(a)(i), there were no microcracks or deformations on the corresponding samples with 10/20 wt. % TiO_2 as shown in Figs. 1(a) (ii) and (iii), respectively. Magnified surface photographs of Fig. 1(b) show the effect of TiO_2 addition. Although the 0% TiO_2 added sample (b)(i) had many cracks, the 10 and 20 wt. % samples (b)(ii) and (iii), respectively, had no cracks. Figs. 2(a), (b) and (c) show polarizing optical photographs of 0, 5 and 10 wt.% TiO_2 added indialite/cordierite glass ceramics, respectively, for comparison of the crystallization conditions. Pure cordierite composition samples [Fig. 2(a)] without TiO_2 addition showed anisotropic crystal growth produced by surface crystallization growing from the surface. The photograph was taken by an inserted sensitive test plate with birefringence of 530 μm. The colored and up pointed head of the elongated crystals showed a color variants which may be due to different phases such as β-quartz solid solutions[30]. The direction of elongation may be *c*-axis and the *c*-axis meets the *a*-axis of another crystal grown from another different rectangular surface. The meeting point of the elongated crystals causes cracks because of the different coefficients of thermal expansion. The expansion of the *c*-axis is negative and that of *a*-axis is positive[29], hence microcracks are formed. On the other hand, Figs. 2(b) and (c) show the crystals precipitated in the glass body. Fig. 2 (b)

shows 5 wt. % TiO_2 added glass ceramics composed of grains with about 400 μm diameter grown from seed crystals of TiO_2, together with spherically grown yellow-colored unknown crystals with about 50 μm diameter. Moreover, Fig. 2(c) shows the 10 wt. % TiO_2 added samples to be composed of many fine spherical crystals with about less than 10 μm diameter. The thin section was not transparent as if the thickness is 30 μm of normal thin section thickness because of the precipitated crystals with too small size. The spherical crystals showed crossed hairs under crossed polars, which indicated the crystallization mechanism from a seed crystal of TiO_2. As the crystallization was performed by volume crystallization, cracks were reduced. Figs. 2(d) and (e) show SEM photographs of crystallized 10 wt. % TiO_2 added samples with different magnifications. The Fig. 2(d) photograph also shows volume crystallization with about 10 μm diameter, which is the same as that observed by the polarizing optical microscope. On the magnified surface of the crystals there are many small dots as shown in Fig. 2(e) which may be the glass phase made clearer by a magnification of photograph 2(d). The deformation of pellets occurred by the glass phase as shown in the previous paper[27)]. In this case, the deformation did not occur because of the small amount of glass phase.

Precipitated phases in the TiO_2 added indialite/cordierite glass-ceramics were identified by the Rietveld method[33)] with the four phases of indialite, cordierite, Al_2TiO_5,

and rutile. Table 2 shows the precipitated phases of the glass-ceramics crystallized between 1200 to 1300 °C/10 h. Indialite was mostly precipitated at lower temperatures such as 1200 °C and decreased from 70% to 37% as the temperature increased to 1300 °C. In contrast, cordierite increased from 30% to 63% as the temperature increased from 1200 to 1300 °C. This shows that indialite transformed to cordierite because indialite is an intermediate metastable phase during crystallization from glass to cordierite[30]. With the addition of 10 wt. % TiO_2, the aluminum titanate phase of Al_2TiO_5 appeared due to the reaction between cordierite and TiO_2, as explained later. The amount of the aluminum titanate phase was 6.0 wt. % at 1200 °C which reduced to 0.32 wt. % at 1300 °C. The maximum value was 32.4 wt. % at 20 wt. % TiO_2 at 1200 °C which decreased to 11.5 wt. % as the temperature increased to 1300 °C. The amount of rutile was reduced to 6.1 wt. % from the original composition of 10 wt. % TiO_2 at 1200 °C. Also, in the case of the 20 wt. % TiO_2 at 1200 °C, the amount of rutile was much reduced to 1.53 wt. % from 20 wt. % and the amounts were increased to 13.58 wt. % as the crystallization temperature increased to 1300 °C. This reduction of the rutile phase might depend on the reaction between TiO_2 and cordierite as shown in the following equation:

$$Mg_2Al_4Si_5O_{18} + TiO_2 = Al_2TiO_5 + \text{unknown phases with MgO and } SiO_2 \quad (1)$$

As some relationships among the various precipitated phases are complicated, they are

explained by the figures, such as Fig. 3(a), (b) and (c), which show precipitated phases as a function of crystallization temperature. The behavior of the amount of cordierite as shown in Fig. 3(b) is different. The amount of cordierite decreased abnormally in the order 10, 0 and 20 wt. % TiO_2 at 1200 °C. This phenomenon is due to the reaction between cordierite and TiO_2 as shown in equation (1). For the 20 wt. % TiO_2 case at 1200 °C, the reaction was predominant to produce the Al_2TiO_5 phase with 32.4 wt. % because of the abundant amount of TiO_2 as shown in Fig. 3(c). Also, the Al_2TiO_5 phase formation reaction further reduced rutile amount with 1.53 wt. %. While in the 10 wt. % case, the same reaction also occurred with 6.0 wt. % Al_2TiO_5 and 6.1 wt. % rutile. As a result, the amount of cordierite with 20 wt. % TiO_2 at 1200 °C became the lowest order and that with 10 wt. % TiO_2 was also affected. In the case of the amount of cordierite at 1300 °C, the order was also affected. More information for the reaction between cordierite and TiO_2 was obtained from this figure, which is active on the 20 wt. % TiO_2 addition at 1200 °C due to decreasing the added TiO_2. The activity decreased with the crystallization temperature because of the increase in residual TiO_2. From this condition, it can be assumed that the Al_2TiO_5 phase was formed more at 1200 °C than at 1300 °C and depended on the amount of TiO_2. At 20 wt. % of TiO_2, the amount of Al_2TiO_5 phase produced at 1200 °C was very large, 32.4%, and the amount of rutile was too low at 2.32%

(see table 2). In the case of 10 wt. % TiO_2, the amount of rutile was 6.1% which showed a low-level reaction due to equation (1).

The XRPD pattern of 20wt. % added TiO_2 crystallized at 1200 ºC/ 10h and analyzed by the Rietveld method is shown in Fig. 4, concerning the equation (1) in this work. The red small circle dotted line (Y_{obs}) and the black solid line (Y_{calc}) in the XRPD patterns are the intensity of diffraction observed and calculated, respectively. The lowest line (Y_{obs}-Y_{calc}) shows the difference between the observed and calculated intensity, and the four short bars lines are the Bragg positions of indialite (indicated by I), cordierite (C), Al_2TiO_5(▼) and rutile (◆) precipitated. The main peaks in the XRPD pattern are indexed as indialite and cordierite without symbols, whose differences are very small as described in a previous paper[30)]. The differences could be observed on the full width at half maximum (FWHM) of the diffraction peaks, especially on the highest peak around 2-theta 29.5º based on the peak splitting due to the phase transition to cordierite phase with low symmetry. The broadening of the peak could be observed in Fig. 5 as follows: the broadenings were larger at 1350 ºC than at 1200 ºC at each value of TiO_2 wt. %, and in order of the wt. % TiO_2. Moreover, some additional peaks of rutile with ◆symbol and Al_2TiO_5 with ▼ symbol due to additional TiO_2 and reaction of equation (1) were observed as secondary phases. The differences of the amount of rutile and aluminum titanate

observed in Fig. 5(a) depended on the precipitated phases for a crystallization time/10h as shown in Table 2 and Fig. 5 as described previously. In the case of the crystallization time/ 20 h, although the amount of precipitated phases was not analyzed by the Rietveld method, we could estimate the value from the XRPD patterns. Other phases containing MgO and SiO_2 due to the equation (1) were not confirmed by the Rietveld analysis.

TiO_2 addition has proved effective for preventing the cracks and the deformation as described above. However, the reinforcement also affected the properties. Fig. 6 shows the density of 0, 10 and 20 wt.% added samples as a function of crystallization temperature. In the case of 0 wt. % added glass ceramics, the densities were located around 2.4 g/cm^3 which is over 95% of the relative density based on the X-ray density D_x = 2.51 for indialite as quoted from ICSD #75634. The densities increased to 2.6 for 10 wt. % and to 2.8 for 20 wt. % addition of TiO_2 having the relative density of 4.23 g/cm^3.

Fig. 7 shows the microwave dielectric properties of 0, 10 and 20 wt. % TiO_2 added samples crystallized at 1200 to 1350 ºC for 10 and 20h. The *Qf* values of pure samples without TiO_2 were the highest at 160× 10^3 GHz at 1350 ºC/20 h which is lower than the 200× 10^3 GHz at 1300 ºC/20 h described in the previous data[27)]. The *Qf* value of 200× 10^3 GHz has previously been presented as ideal data depending on the sample condition, the synthesis condition, measurement method *etc*. The 0% added TiO_2

cordierite glass was crystallized with cracks as previously described because of surface crystallization. So, the *Qf* values fluctuated as reported in our previous paper[28]. This work produced a series of samples with added TiO_2 of 0, 10 and 20 wt. %. In the case of 0 wt. % TiO_2 addition, the samples were reproduced as presented in the previous paper[27]. The reproduced samples in this work were not so severely cracked compared with the previous ones. Most of the *Qf* properties also did not fluctuate as shown in Fig. 7(a). Although the TiO_2 addition had a significant effect in reducing the previously described cracking and in adjusting the *TCf* to near-zero ppm/°C, as described later, the *Qf* values were decreased from 140 x10^3 GHz for 0 wt. % to 40x10^3 GHz for 20 wt. %TiO_2 addition as shown in Fig. 7(a). Usually, although high purity materials show high *Qf*, impurities and secondary phases reduce the *Qf*[1,8] the *Qf* values of 0 wt. % TiO_2 added sample crystallized for 10 h typically increased from 1200 to 1300 °C in the initial stage and decreased over the temperature. In the initial stage, sintering affected the *Qf* values due to increasing the density as shown in Fig. 6. In the continuous stage, the decrease of indialite affected the *Qf* values due to phase transformation to cordierite as shown in Table 2 and Fig. 3. Indialite, with a disordered structure, showed a higher *Qf* than cordierite with an ordered structure, as presented previous papers[28]. The *Qf* highest point of 0 wt. % TiO_2 addition sintered at 1350 °C/20h did not show the decreasing tendency due to

fluctuation of crystallization conditions as described before[27-28]. In the case of 20wt. % added TiO_2, the Al_2TiO_5 phase affected the *Qf* values, which is precipitated mostly at 1200 °C crystallization and then decreased as temperature rising at 1350 °C. This phase changes are clear from XRPD pattern as shown in Fig. 5(b). The diffraction peaks are disappeared which is corresponds to (▼) Al_2TiO_5. The diffraction 101 and 230 peaks (▼) of Al_2TiO_5 disappeared entirely and the 110 peak (◆) of rutile became strongest at 1350 °C/20 h. In the case of 1350 °C/10 h, the peaks of Al_2TiO_5 remained, is weak.

Fig. 7(b) shows the dielectric constant ε_r of 0, 10 and 20 wt. % TiO_2 added as a function of crystallization temperature. In the case of 0 wt. % TiO_2 addition, the ε_r values in the range of 1200 to 1350 °C were almost exactly 4.5, although indialite phase transformed to cordierite, as shown in Table 2 and Fig. 3. In the previous data[27], ε_r was 4.7 which might be due to measuring error. The ε_r values were increased to 5.8 and 6.8 by the addition of 10 and 20 wt. % TiO_2, respectively, due to the addition of TiO_2 with $\varepsilon_r = 104$[40, 41]. In the case of 20 wt. %/20 h, the ε_r values increased as shown in Fig. 7(b). At 1200 °C/20 h, the ε_r value was 6.9 due to the Al_2TiO_5 with $\varepsilon_r = 10.3$[42] precipitated by the reaction of equation (1) as the amount of Al_2TiO_5 was more and that of rutile was less as estimated by the diffraction pattern of Fig.5(b). The ε_r values increased significantly to 12.9 as shown in Fig. 7(b), with increasing crystallization temperature from 1200 to 1350

°C/20 h. At the 1350 °C/20 h, the Al_2TiO_5 diffraction peaks disappeared and the rutile peak was maximum as shown in Fig. 5(b). However, in the case of 20 wt. %/10 h, the Al_2TiO_5 phase slightly less about 11.5 wt. % as shown in Fig. 5(a) and Table 2. Hence, the ε_r of 1300 °C/10h was lower than that of 20 h. The XRPD figures show systematically the amount of Al_2TiO_5 and rutile. The diffraction peaks 101 and 230 of Al_2TiO_5 decreased with increase in the temperature from 1200 to 1350 °C as shown in Fig. 5(a) and (b). Also the intensity of 110 peak of rutile increased.

Fig. 7(c) shows the temperature coefficient of the resonance frequency (*TCf*) of 0, 10 and 20wt. % TiO_2 added as a function of crystallization temperature. In the case of zero addition of TiO_2, the *TCf* values did not change from around -28 ppm/°C, although the phases transferred from indialite to cordierite. So, the *TCf* of both compounds were similar to -28 ppm/°C. The effects of TiO_2 are two-fold, as described before. Here, TiO_2 with a positive *TCf* of +450 ppm/°C[35)] was added to adjust the *TCf* value. In the case of 10 and 20 wt. % TiO_2 samples crystallized at 1200 °C/10/20 h, the *TCf* value of 10 wt. % with -13/-8 ppm/°C was higher than that of 20 wt. % with -29/-20 ppm/°C which was not improved by the TiO_2 addition. As shown in Table 2 and Fig. 3(c), the TiO_2 reacts with cordierite according to the equation (1), forming the Al_2TiO_5 phase. The reaction in the 20 wt. % addition case was more active than that in the 10 wt. %. The amount of Al_2TiO_5

phase in 20 wt. % addition was 32.4 wt. % and that of rutile was only 1.53 wt. %, so the TCf value of -29/-20 ppm/°C was not improved. On the other hand, in the case of 10 wt. % addition, as the amount of rutile of 6.1 wt. % was higher than that of the 20 wt. %, the *TCf* value was improved to -13/-8 ppm/°C. The amount of Al_2TiO_5 in the case of 10 wt. % added was 6.0 wt. % and reduced to 0.32 wt. % at 1300 °C. However, the amount of rutile phase increased to 10.2 wt. % which corresponded to the addition of the TiO_2 amount 10 wt. %. The *TCf* values increased to 14/15 ppm/°C at 1350 °C/10/20 h through the -2/-8 ppm/°C at 1250 °C, and were expected to be near 0 ppm/°C at around 1270 °C. In the case of 20 wt. % addition, the *TCf* values drastically increased to 210/205 ppm/°C at 1350 °C/10/20 h as the amount of rutile increased from 1.53 to 13.58 wt. %. The *TCf* value was adjusted to 0 ppm/°C at around 1230 °C.

4. Conclusion

The microwave dielectric properties of indialite/cordierite glass-ceramics have been improved by the addition of TiO_2 for micro/millimeter wave applications. There are two problems with material such as deformation and cracks, which are based on the glass phases and anisotropic crystal growth, respectively. The addition of TiO_2 allowed volume crystallization composed by spherical crystals with about 20 μm diameter scale, which reduced the deformation and cracks by surface crystallization with anisotropic crystal

growth. These phenomena were observed by a polarizing microscope. Based on the precipitated phases analyzed by the Rietveld method, the TiO_2 addition reacted with cordierite forming Al_2TiO_5. The number of precipitated phases with different results such as indialite, cordierite, Al_2TiO_5 and rutile could be explained using the reaction between TiO_2 and cordierite. The microwave dielectric properties of the composite are presented. *Qf* decreased with the amount of TiO_2 addition and the density and precipitated phases also affected the *Qf* value. The ε_r values increased with the addition of TiO_2 and in the case of 20 wt. % added TiO_2 the ε_r increased drastically from 6.7 to 12.9 depending on the amount of Al_2TiO_5 (ε_r = 10.3) and rutile (ε_r = 104). The *TCf* values in the case of 10/20wt. % TiO_2 added were improved near 0 ppm/°C crystallized at 1270/1230 °C/10 h, respectively. The values of 10/20 wt. % TiO_2 addition is drastically increased to 210/205 ppm/°C at 1350 °C depending on the amount of rutile.

Acknowledgments

The authors are grateful to Doctoral Student Jukka Pekka Ranta, Marko Moilanen, and Technician Sari Forss in the Mining School in the University of Oulu for observation by polarizing microscope, measurement of chemical composition and fabrication of thin sections, respectively. Moreover, the authors are grateful to President Sadahiko Suzuki

of Marusu Glaze Co., Ltd. for the indialite/cordierite powder and Director Masato Mitsumatsu and Head of Ceramic Technology Group Kenji Ito in the Seto Ceramic Research Institute for the fabrication of the ceramics. Visiting professor Hitoshi Ohsato is grateful to JSPS KAKENHI Grant Numbers 22560673, 25420721, JP16K06735 and Nokia Foundation 2016 for supporting this work for the Nokia Visiting Professors Project 201700003. Professor Heli Jantunen and Dr. Jobin Varghese are grateful to European Research Council Project No. 24001893 for financial assistance.

References

1) H. Ohsato, “Millimeter-Wave Materials”, in Microwave Materials and Applications *ed*. M. T. Sebastian, R. Ubic, and H. Jantunen (Wiley, New York, 2017), Vol. 1, Chap. 5.

2) NTT DOCOMO, INC. White Paper 5G Evolution and 6G, January 2020 https://www.nttdocomo.co.jp/english/binary/pdf/corporate/technology/whitepaper_6g/DOCOMO_6G_White_PaperEN_20200124.pdf#page=1 [Accessed:2020-0616]

3) H. Holma, A. Toskala, and T. Nakamura, “5G technology: 3GPP new radio,” Wiley, Dec. 2019. S. Suzuki and M. Asada, “Terahertz Wireless Communications using Electronic Devices”, MWE2014 Microwave Workshops Digest, pp 195-198, 2014.

4) M. D. Hill and D. B. Cruickshank, Ceramic materials for 5G wireless communication systems, Am. Ceram. Soc. Bulletin, 98(6), 20-25, (2019).

5) M. T. Sebastian: Dielectric Materials for Wireless Communication. Amsterdam: Elsevier. 2008; ISBN-13:978-0-08-045330-9

6) H. Ohsato: Microwave Dielectrics with Perovskite-Type Structure. In: Pan L, Zhu G, editors: Perovskite Materials - Synthesis, Characterization, Properties, and Applications. Rijeka, Croatia: INTECH; 2016. P.281-330. ISBN 978-953-51-4587-5. Open Access: http://cdn.intechopen.com/pdfs-wm/49723.pdf [Accessed:2019-08-15]

7) T. Tsunooka, H. Sugiura, Y. Higashida, T. Fukui, H. Okawa and Y. Iwata, Low-permittivity Ceramic Dielectrics, JFCC Review, 4, 72-81 (1992).
8) M. T. Sebastian, R. Ubic, H. Jantunen: Low-loss dielectric ceramic materials and their properties. International Materials Review. 60, 392-412 (2015).
9) T. Tsunooka, M. Andou, Y. Higashida, H. Sugiura and H. Ohsato, Effects of TiO_2 on sinterability and dielectric properties of high-*Q* forsterite ceramics, J. Eur. Ceram. Soc., 23(14), 2573-2578, (2003).
10) T. Tsunooka, H. Sugiyama, K. Kakimoto, H. Ohsato, and H. Ogawa, Zero Temperature Coefficient τf and Sinterability of Forsterite Ceramics by Rutile Addition, J. Ceram. Soc. Jpn. **112**, (2004) S1637-S1640.
11) T. Sugiyama, T. Tsunooka, K. Kakimoto and H. Ohsato, Microwave dielectric properties of forsterite-based solid solutions, J. Eur. Ceram. Soc., 26, 2097-2100 (2006.3).
12) H. Ohsato, T. Tsunooka, T. Sugiyama, K. Kakimoto and H. Ogawa, Forsterite ceramics for millimeterwave dielectrics, J. Electroceramics, 17, 445-450 (2006).
13) H. Ohsato, M. Ando and T. Tsunooka, Synthesis of Forsterite with High *Q* and Near Zero *TCf* for Microwave/Millimeterwave Dielectrics, J. Korean Ceram. Soc., 44(11), 597~606(2007).
14) M. Ando, K. Himura, T. Tsunooka, I. Kagomiya, and H. Ohsato, Synthesis of High-Quality Forsterite, Jpn. J. Appl. Phys. **46**, 7112-7116 (2007).
15) M. Ando, H. Ohsato, I. Kagomiya, and T. Tsunooka, Quality factor of forsterite for Ultrahigh Frequency Dielectrics Depending on Synthesis Process, Jpn. J. Appl. Phys. **47**, 7729-7731 (2008).
16) Y. Guo, H. Ohsato and K. Kakimoto, Characterization and dielectric behavior of willemite and TiO_2-doped willemite ceramics at millimeter-wave frequency, J. Eur. Ceram. Soc., 26, 1827-1830 (2006.3).
17) M. Ando, H. Ohsato, D. Igimi, Y. Higashida, A. Kan, S. Suzuki, Y. Yasufuku, and I. Kagomiya, Low-temperature sintering of silica‐boric acid-doped willemite and microwave dielectric properties, Jpn. J. Appl. Phys. **54**, 10NE03-1-6 (2015).
18) H. Ohsato, M. Terada, and K. Kawamura, Fabrication Conditions of Diopside for Millimeterwave Dielectrics, Jpn. J. Applied Physics, 51(9), (2012) 09LF02-1-4.

19) H. Ohsato, I. Suzuki, I. Kagomiya, Crystal structure and microwave dielectric properties of alfa-$(Ca_{1-x}Sr_x)SiO_3$ (x = 1 and 0.8) ring silicates for millimeter-wave applications, Materials Research Bulletin, 96 (2017) 115-120.
20) L. Pauling, The nature of silicon-oxygen bonds, Am. Mineral., 65,321-323, 1980.
21) M. Terada, K. Kawamura, I. Kagomiya, K. Kakimoto, and H. Ohsato, Effect of Ni substitution on the microwave dielectric properties of cordierite, J. Eur. Ceram. Soc. **27**, 3045-3148 (2007).
22) H. Ohsato, I. Kagomiya, M. Terada, and K. Kakimoto, Origin of improvement of Q based on high symmetry accompanying Si–Al disordering in cordierite millimeter-wave ceramics, J. Eur. Ceram. Soc., 30, 315-318 (2010).
23) G. V. Gibbs, The polymorphism of cordierite I: the crystal structure of low cordierite, Am. Mineral. 51 (1966) 1068-1087.
24) W. Schreyer and J. F. Schairer, Phase diagram No. 2533, J. Pertol., 2, (1961) 324-406.
25) T. Sugimura, H. Ohsato and Y. Nakai, The metastable Zn-indielitecrystallozed out from the glasses in the ternary system ZnO-Al_2O_3-SiO_2, Yogyo-Kyokai-Shi, 82(1), 48-54 (1974).
26) H. Ohsato, J. S. Kim, A.Y. Kim, C. I. Cheon, and K.W. Chae, Millimeter-Wave Dielectric Properties of Cordierite/Indialite Glass Ceramics, Jpn. J. Appl. Phys. **50**, 09NF01-1-5 (2011).
27) H. Ohsato, J.S. Kim, C.I. Cheon, I. Kagomiya, Millimeter-wave dielectrics of indialite/cordierite glass ceramics: Estimating Si/Al ordering by volume and covalency of Si/Al octahedron. J. Ceram. Soc. of Jpn, **121**, 649-654 (2013).
28) I. Ogata, K. Mizutani, K. Makino and Y. Kobayashi, Analysis of the low thermal expansion mechanism of preferably oriented, DENSO Tech. Rev. 13 (2008) 112-118, (Japanese).
29) H. Ohsato, J. S. Kim, C.-Il Cheon and I. Kagomiya, Crystallization of indialite/cordierite glass ceramics for millimeter-wave dielectrics, Ceramics International, 41 (2015) S588-S595. doi:10.1016/j.ceramint.2015.03.14.
30) B. W. Hakki, P. D. Coleman, A dielectric resonator method of measuring inductive in the millimeter range, IRE Trans. Microw. Theory Tech., (MTT)-8 (1960) 402–410.
31) Y. Kobayasi, M. Kato, Microwave measurement of dielectric properties of low-loss materials by the dielectric resonator method, IEEE Trans.Microw. Theory Tech., (MTT)-33 (1985) 586–592.

32) Fullprof Software by Juan Rodriguez-Carvajal in France,<http://www-llb.cea.fr/fullweb/powder.htm>. [Accessed:2020-04-01]
33) Table of dielectric constants on Yamamoto Electric Industrial CO., LTD http://www.ydic.co.jp/technology/table.html#Anchor_t [Accessed:2020-04-01]
34) L. Li, C. H. Lui, J Y. Zhu and X. M. Chen. `B_2O_3- modified fused silica microwave dielectric materials with ultra-low dielectric constant. J. Eur. Cer. Soc. 2015, 35 (6), 1799-1805.
35) L. Li, Y. Fang, Q. Xiao, Y. J. Wu, N. Wang and X. M. Chen. `Microwave dielectric properties of fused silica prepared by different approaches`. Intl. J. Appl. Ceram. Techn. 2014, 11, 193- 199.
36) Y. Fang, L. Li, Q Xiao, X. M. Chen. 'Preparation and microwave dielectric properties of cristobalite ceramics. Ceram. Intl. 2012, 38, 4511-4515
37) B. J. Jeong, M-R. Joung, S-H. Kweon, I-S. Kim, S. Nahm, J. W. Choi, S-J. Hwang. Effect of Bi_2O_3 doping on the sintering temperature and microwave dielectric properties of $LiAlSiO_4$ ceramics. J. Amer. Ceram. Soc. 2012, 95, 811-813.
38) S. George, P. S. Anjana, V. N. Deepu, P. Mohanan and M. T. Sebastian. Low temperature sintering and microwave dielectric properties of Li_2MgSiO_4 ceramics. J. Amer. Ceram. Soc. 2009, 92, 1244-1249.
39) T. Okamura, and T. Kishina. Dielectric properties of rare earth added cordierite at microwave and millimeterwave frequencies. Jpn. J. Appl. Phys. 1998, 37, 5364-5366.
40) M. Maeda, T. Yamamura, T. Ikeda, Dielectric characteristics of several complex oxide ceramics at microwave frequencies. Jpn. J. Appl. Phys. Supl., 1987, 26-2, 76-79.
41) A. Templeton, X. Wang, S. J. Penn, S. J. Webb, L. F. Cohn, N. Mc N. Alford . Microwave dielectric loss of titanium oxide. J. Amer. Ceram. Soc., 2000, 83, 95-100.
42) K. P. Surendran, N. Santha, P. Mohanan and M. T. Sebastian. Temperature stable low permittivity ceramic dielectrics in $(1-x)ZnAl_2O_4$-$xTiO_2$ system for microwave substrate applications. Eur. Phys. J. B, 2004, 41, 301-306.

Table captions:

Table 1. Comparison of density and microwave dielectric properties of present TiO_2 added volume crystallized indialite/cordierite glass ceramics with that of reported

materials with ε_r > 5 and Qf < 20*10^{3}GHz (excluded the materials with less durability).

Table 2. Amount of precipitated phases for different levels of TiO_2 added indialite/cordierite glass ceramics crystallized 1200 to 1300 ^oC/10 h analyzed by Rietveld method.

Figure captions:

Fig. 1. Effect of TiO_2 addition for indialite/cordierite glass ceramics: (a) and (b) are photographs by Olympus optical microscope. i) no addition TiO_2 with cracks and deformation, ii) 10 wt% and iii) 20 wt% TiO_2 addition without cracks and deformation.

Fig. 2. Optically polarized microscopic thin section images of no addition TiO_2 indialite/cordierite glass ceramics crystallized from surface (a), 7 wt. % TiO_2 addition crystalized from body (b), and 10 wt. % TiO2 addition precipitated spherical crystals with ca. 10 μm. SEM micrographs of 10 wt. % of TiO_2 addition with grains of ca. 10 μm (d) and with glass phase (e) on indialite/cordierite glass ceramics.

Fig. 3. Precipitated phases of indialite (a), cordierite (b) and Al2TiO5 and rutile (c) from different TiO_2 added glass as a function of crystallization temperature presented in Table 2.

Fig. 4. XRPD pattern analyzed by Rietveld method of indialite/cordierite glass ceramics crystallized at 1200 ^oC/10 h. Main peaks are confirmed as indialite/cordierite and Al_2TiO_5 (▼) and rutile (◆) are precipitated. The red small circle (Y_{obs}) and black solid line (Y_{calc}) are intensity of diffraction observed and calculated, respectively. The lowest line (Y_{obs}-Y_{calc}) is the difference between observed and calculated intensity, and four short bars lines are Bragg positions of indialite, cordierite, Al_2TiO_5 and rutile.

Fig. 5. Retiveld refined XRPD patterns of different TiO_2 added indialite/cordierite glass ceramics depending on the crystallization temperature and hours of 10 and 20 h. Precipitated amount of titanium aluminate and rutile should be estimated on crystallization time of 20 h as shown in the case of 10 h on Table 2 and Fig. 3.

Fig. 6. Density of different TiO_2 added indialite/cordierite glass ceramics as a function of crystallization temperature.

Fig. 7. Microwave dielectric properties of different TiO_2 added indialite/cordierite glass ceramics as a function of crystallization temperature and times.

Table 1. Comparison of density and microwave dielectric properties of present TiO_2 added volume crystallized indialite/cordierite glass ceramics with that of reported materials with ε_r > 5 and Qf < 20*10^{3}GHz (excluded the materials with less durability).

Materials	ρ (g/cm^{-3})	ST/CT (°C)	ε_r	$Qf\times10^3$ (GHz)	f (GHz)	TCf (ppm/°C)	References
0ICGC	2.36	1200 / 10	4.6	133.3	13.7	-28	Present work
0ICGC	2.41	1250 / 10	4.5	139	13.8	-29	Present work
0ICGC	2.42	1300 / 10	4.5	145.94	13.8	-29	Present work
0ICGC	2.45	1350/10	4.5	118.25	13.8	-29	Present work
0ICGC	2.41	1200 / 20	4.5	105.8	13.8	-29	Present work
0ICGC	2.44	1250 / 20	4.5	136.65	13.8	-29	Present work
0ICGC	2.45	1300 / 20	4.4	139.4	13.8	-28	Present work
0ICGC	2.43	1350 / 20	4.5	160	13.7	-28	Present work
10ICGC	2.61	1200 / 10	5.8	68.8	12.6	-13	Present work
10ICGC	2.60	1250 / 10	5.7	70.2	12.6	-2.0	Present work
10ICGC	2.60	1300 / 10	6.0	69.9	12.3	-12	Present work
10ICGC	2.60	1350 / 10	6.3	31	12.1	14	Present work
10ICGC	2.60	1200 / 20	5.9	62.8	12.4	-8	Present work
10ICGC	2.61	1250 / 20	5.8	88	12.5	-8	Present work
10ICGC	2.70	1300 / 20	5.8	64	12.5	11	Present work

10ICGC	2.60	1350 / 20	6.3	14.24	12.1	15	Present work
20ICGC	2.76	1200 / 10	6.7	22.85	11.7	-29	Present work
20ICGC	2.74	1250 / 10	7.2	38.46	11.5	6.7	Present work
20ICGC	2.80	1300 / 10	8.7	40.15	10.7	97	Present work
20ICGC	2.77	1350 / 10	10.5	41	9.7	210	Present work
20ICGC	2.72	1200 / 20	6.9	26.3	11.7	-20	Present work
20ICGC	2.79	1250 / 20	7.3	47.26	11.4	16	Present work
20ICGC	2.74	1300 / 20	9.1	45.96	10.3	160	Present work
20ICGC	2.71	1350 / 20	12.9	54.86	9.7	205	Present work
$0.2B_2O_3$-$0.8SiO_2$	-	1100	3.6	70.6	-	-	34
SiO_2 (solid state method)	-	1100	3.7	44.3		-15	35
SiO_2	-	1650	3.8	80.4	-	-16	36
$LiAlSiO_4$+15 wt% Bi_2O_3	-	900	4.3	62.4	-	-16	37
LiAlSiO4	-	1350	4.8	36	-	8	38
(cordierite) $Mg_2Al_4Si_5O_{18}$+7 wt% Yb_2O_3	-	1420	4.9	112	18	-	39

0, 10, 20 ICGC = 0, 10, 20 wt.% TiO_2 added indialite/cordierite glass ceramics

crystallized ρ = density; ST/CT= sintering/crystallization temperature; ε_r = relative permittivitiy; Qf = quality factor * resonant frequency; *f* = resonant frequency; *TCf* = temperature coefficient of resonant frequency

Table 2. The amount of precipitated phases for different levels of TiO_2 added indialite/cordierite glass ceramics crystallized 1200 to 1300 °C/10 h analyzed by Rietveld method.

Compounds	0 wt% TiO_2 wt%		10wt% TiO_2 wt%		20 wt% TiO_2 wt%		
	1200°C	1300°C	1200°C	1300°C	1200°C	1250°C	1300°C
1. Indialite	70(3)	37(1)	47.3(7)	26.4(1)	37.3(2)	22.88(6)	15.52(5)
2. Cordierite	30(2)	63(1)	40.6(3)	63.1(4)	28.8(5)	47.0(3)	59.4(4)
3. Al_2TiO_5	-	-	6.0(2)	0.32(0)	32.4(3)	21.8(1)	11.5(1)
4. Rutile	-	-	6.1(1)	10.2(2)	1.53(6)	8.27(6)	13.58(8)

Figure 1

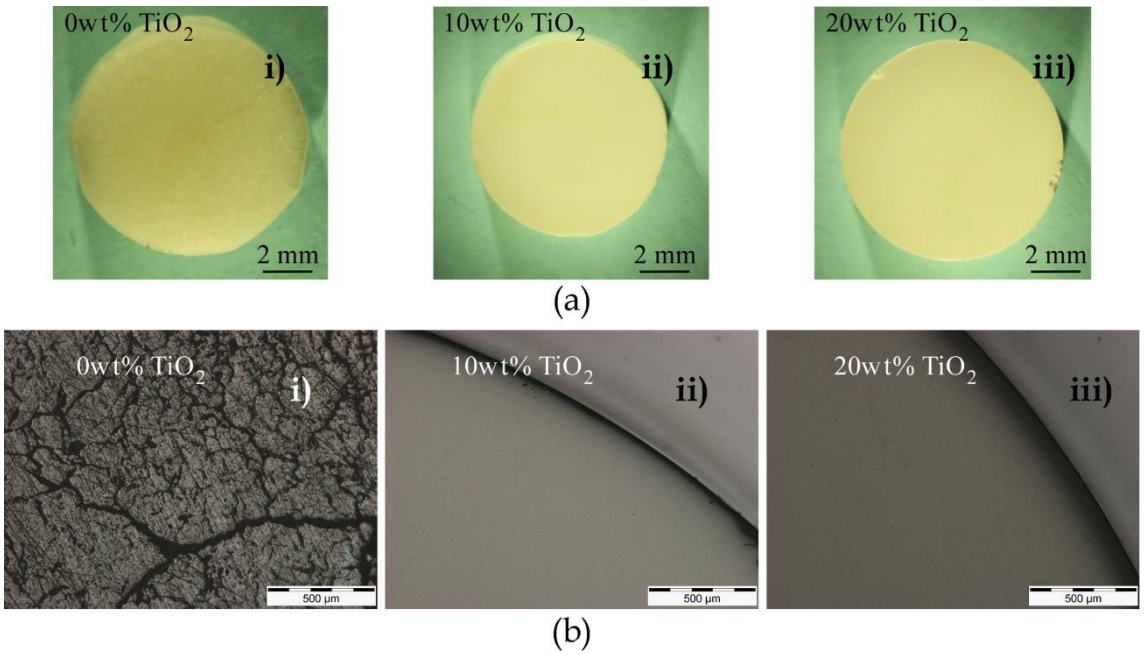
0wt% TiO2
i)
2 mm
10wt% TiO2
ii)
2 mm
20wt% TiO2
iii)
2 mm
(a)
0wt% TiO2
i)
500 µm
10wt% TiO2
ii)
500 µm
20wt% TiO2
iii)
500 µm
(b)

Figure 2

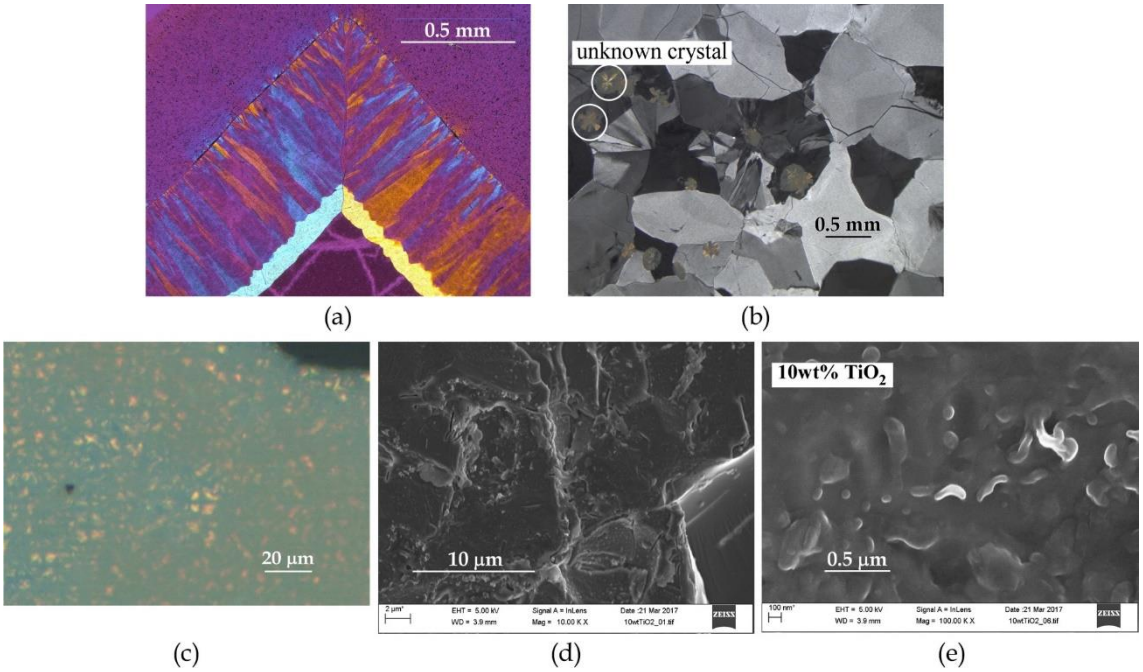

Figure 3

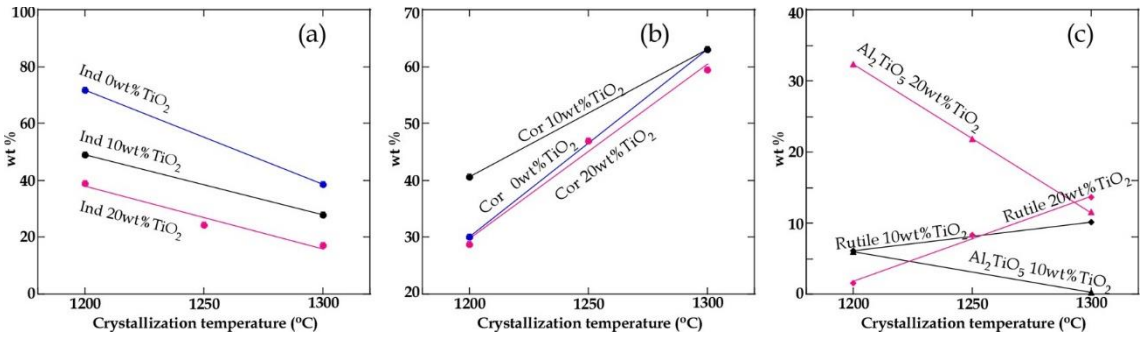

Figure 4

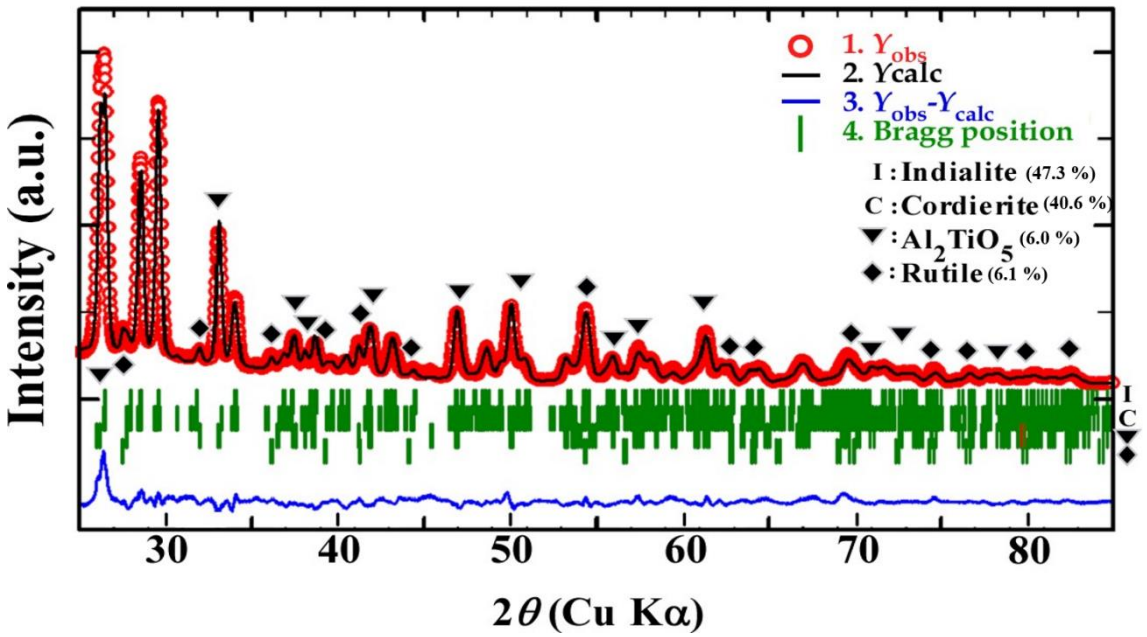
1. Y_{obs}
2. Ycalc
3. Y_{obs}-Y_{calc}
4. Bragg position
I : Indialite (47.3 %)
C : Cordierite (40.6 %)
▼ : Al_2TiO_5 (6.0 %)
◆ : Rutile (6.1 %)
Intensity (a.u.)
30
40
50
60
70
80
2θ (Cu Kα)
I
C
▼
◆

Figure 5

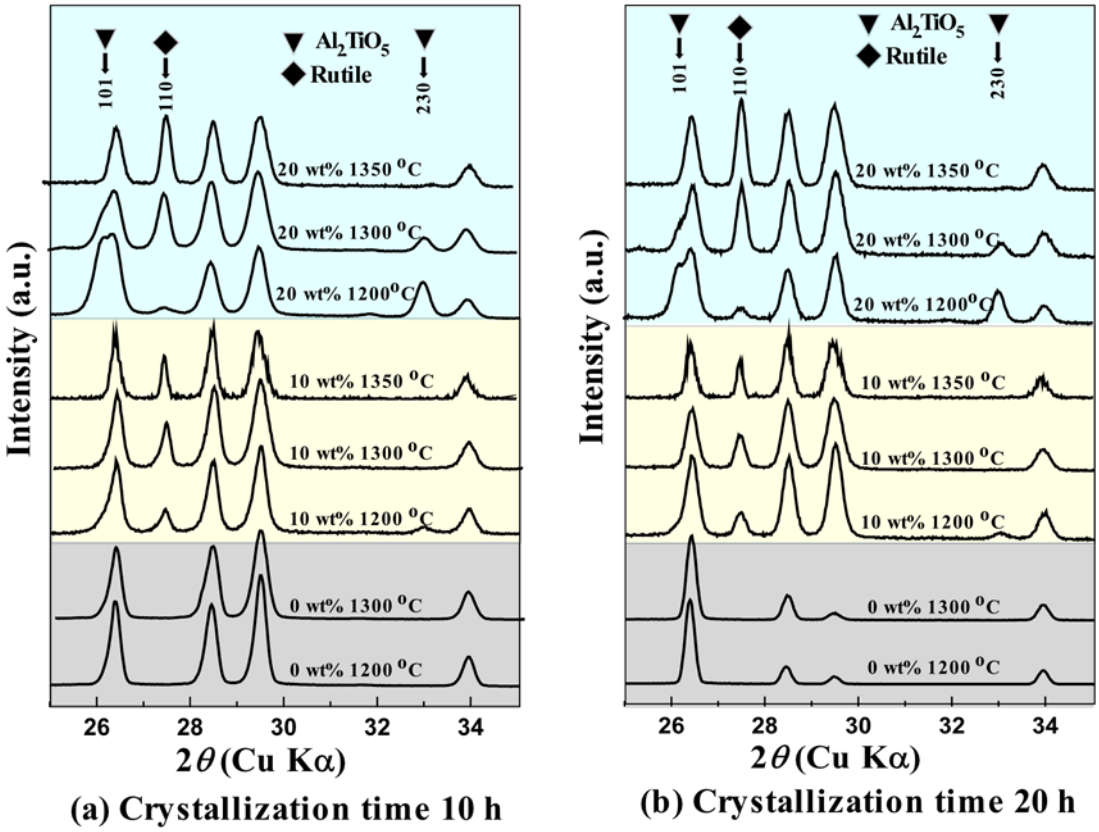
101
110
230
Al2TiO5
Rutile
20 wt% 1350 °C
20 wt% 1300 °C
20 wt% 1200°C
10 wt% 1350 °C
10 wt% 1300 °C
10 wt% 1200 °C
0 wt% 1300 °C
0 wt% 1200 °C
Intensity (a.u.)
26
28
30
32
34
2θ (Cu Kα)
(a) Crystallization time 10 h
(b) Crystallization time 20 h

Figure 6

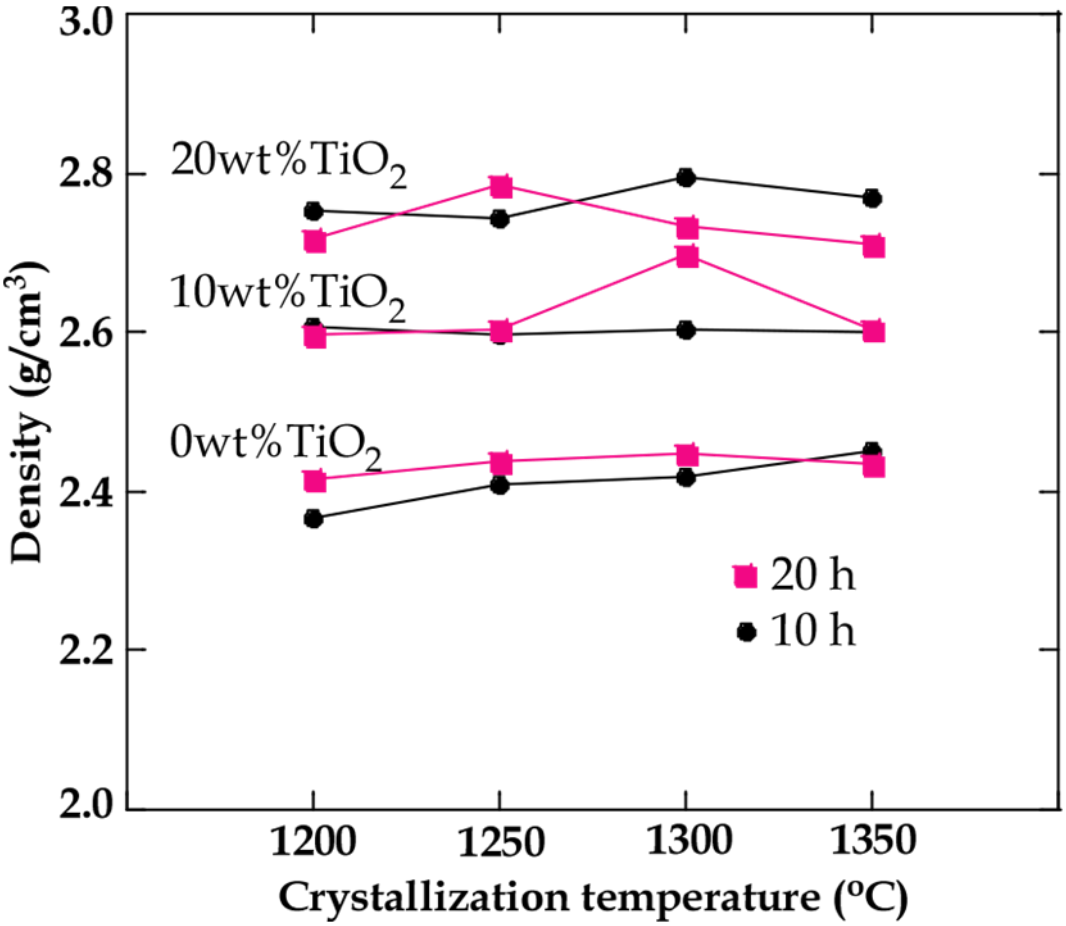
3.0
2.8
2.6
2.4
2.2
2.0
Density (g/cm^3)
20wt%TiO$_2$
10wt%TiO$_2$
0wt%TiO$_2$
20 h
10 h
1200
1250
1300
1350
Crystallization temperature (°C)

Figure 7

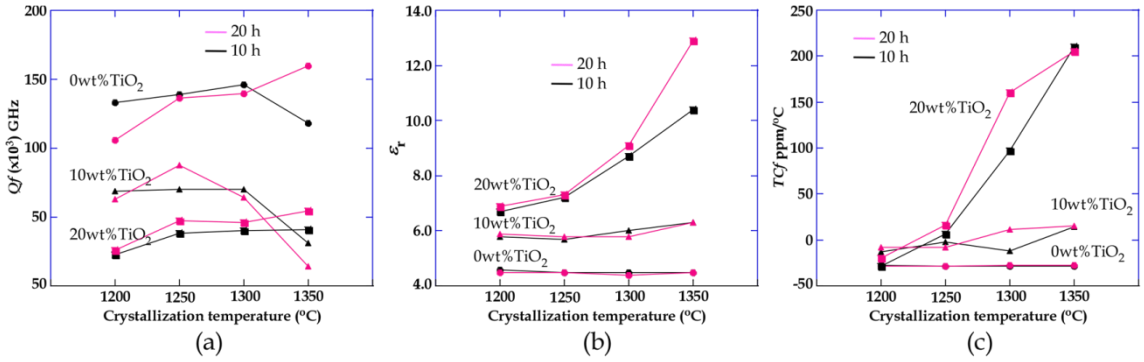
200
150
100
50
Q/f (x10³) GHz
20 h
10 h
0wt%TiO2
10wt%TiO2
20wt%TiO2
1200
1250
1300
1350
Crystallization temperature (°C)
(a)
14.0
12.0
10.0
8.0
6.0
4.0
εr
20 h
10 h
20wt%TiO2
10wt%TiO2
0wt%TiO2
1200
1250
1300
1350
Crystallization temperature (°C)
(b)
250
200
150
100
50
0
-50
TCf ppm/°C
20 h
10 h
20wt%TiO2
10wt%TiO2
0wt%TiO2
1200
1250
1300
1350
Crystallization temperature (°C)
(c)